Analysis and Characterization of End-User Equipment Noise Signals for Power Line Communication Applications

M. F. Akorede[1], G. I. Eguaosa[2*], C. T. Thomas[3], E. Pouresmaeil[4], S. Taheri[5]

[1, 2] Department of Electrical and Electronics Engineering, University of Ilorin, Nigeria
[2] Eko Electricity Distribution Company, Lagos, Nigeria
E-mail: gladness.eguaosa@ekedp.com
[3] Department of Electrical and Information Engineering, Achievers University, Owo, Nigeria
[4] Department of Electrical Engineering and Automation, Aalto University, Espoo, Finland
[5] Department of Computer Science and Engineering, Université du Québec en Outaouais, Gatineau, Canada

Abstract — Power Line Communication (PLC) is the use of the existing public and private mains power wiring for the transmission of telecommunication signals (data). PLC technology is used for a variety of functions, such as computer networking, utility control systems and smart grid. However, one of the predominant challenges faced by PLC is noise, often provoked by end-user equipment. In this paper, an algorithm to characterize different noise types - peculiar to PLC - is developed. Twelve devices across three load classes (residential, commercial and industrial) are chosen for the study. Experimental measurements are carried out on the devices to capture signals of interest. The characterization process in the work is a combined approach of the Power Spectral Density (PSD) and time stream. PSD analysis is carried out on the captured noise signals using the Welch's PSD estimation technique. The PSD and other parameters obtained from the time stream are used for the characterization process. Major findings show that most of the devices exhibited either colored background noise, periodic impulsive noise synchronous with the mains or periodic impulsive noise asynchronous with the mains. The outcome of this research will be useful for development and deployment of power line technologies in a manner that mitigates noise problems.

Keywords — Power line communication; Noise signal characterization; End-user equipment; Power spectral density.

1. INTRODUCTION

Power Line Communication (PLC) involves the use of the existing power line conductors deployed for transmission of electric power as a medium for telecommunication. It offers a convenient and inexpensive medium for high-speed data transmission [1-3]. PLC is useful for remote controlling, energy metering, protection, data acquisition, maintenance and customer feedback relations. Other areas of application include lighting control, solar panel monitoring, in-home video distribution, electric cars, and smart energy management technology [4].

In addition of being very useful as an exclusive communication system for electricity networks, PLC - generally - presents a more stable communication system. It also provides a secure system from hackers, and has a higher reliability value than mobile wireless communication [3, 5]. In urban areas, attenuation losses of wireless communications are high, and signal strength is low or non-existent [6]. Interference of signals can occur in these areas due to the presence of physical objects like high rise buildings, geographical terrain, topology, material make up of structures, climatic conditions, etc. Unlike wireless telecommunications where the communication signal is prone to diffraction, reflection and scattering, PLC does not have limitations of line-of-sight and short transmission range [4]. Also, since almost every

218

environment utilizes the grid electricity, using PLC as mainstream communication system would be greatly valued.

Typical PLC framework is illustrated in Fig. 1 where electrical energy is transmitted at 50/60 Hz, while communication signals are transmitted at frequencies between 3 kHz and 300 GHz [7]. However, for practical PLC communication, operating frequency range is between 3 kHz and 250 MHz. Since both electrical and communication signals are transmitted over the same channel (power lines), the line traps (also known as wave traps) work as a low pass filter, allowing only the electrical signals to pass through. The coupling devices and capacitors are used for filtering purposes, after which the communication signal is obtained. The signal is then sent over coaxial cables from the switchyard to the communications room and from there to various end-users.
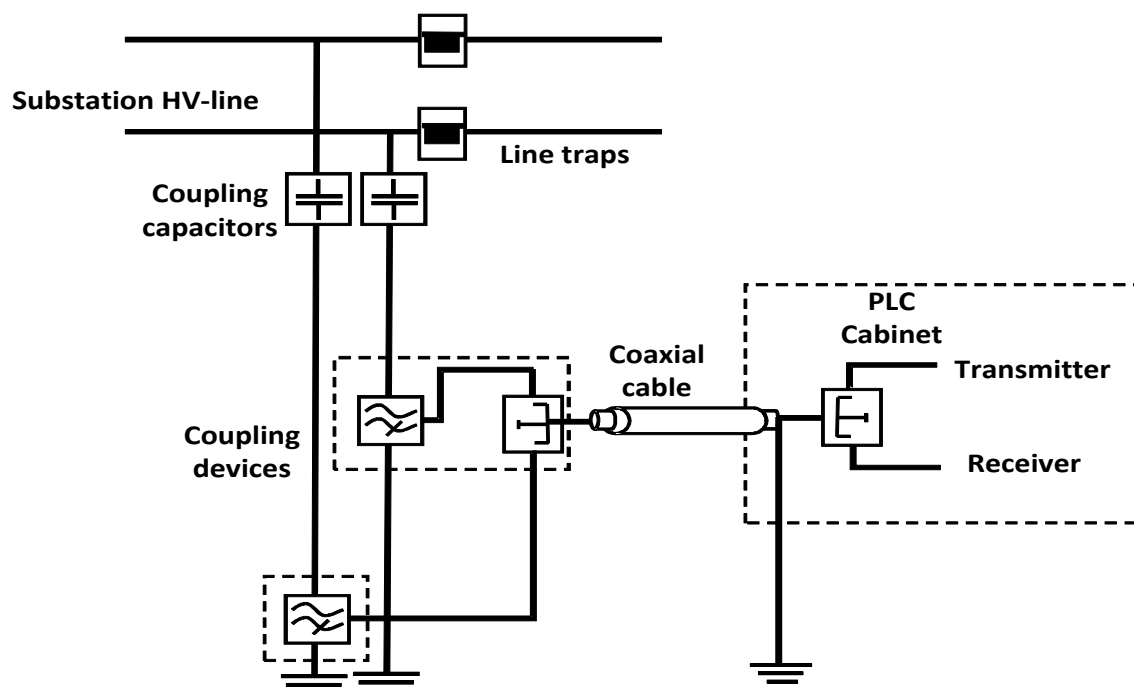

Fig. 1. PLC structure showing interface of station with PLC equipment for a 2-phase coupling device setup.

Despite the advantages that PLC presents, it is faced with several challenges. These challenges happen because the power lines do not provide a favorable environment for communication signals since they were originally designed for electrical power. The characteristics of the power lines that need to be contended with are: time-varying frequency, dependent channel attenuations and reflections from non-terminated points that result in multipath fading and various types of noise [8]. Noise in PLC is generally influenced by the nature of several end-user equipment being connected on the power network. Activities - such as plug-in/out and switching - disturb the line parameters and corrupt the message/data sent across the medium. The fact that the activities of these devices are unpredictable poses a greater challenge. Noise characterization is essential in application of PLC systems, as they provide the impact of the medium on the transmitted communication signal [9]. Since there are various end-user equipment and several types of noise associated with them; proper understanding of these noise types as well as the likely sources becomes necessary. This is the crux of this research.

2. PLC CLASSIFICATION AND NOISE TYPES

2.1. Classification of PLC

PLC is generally classified - as illustrated in Fig. 2 - based on three parameters: application, power line voltage and operating frequency. In a more specific sense, PLC is classified as indoor broadband (BB) PLC and outdoor narrowband (NB) PLC. BB-PLC operates with high data rates of up to 100 Mbps [10], and frequency range of 1.8-250 MHz. BB-PLC is suitable for short distance applications such as home area networks that interconnect smart appliances with smart meters for energy consumption profiling and automatic control [11].
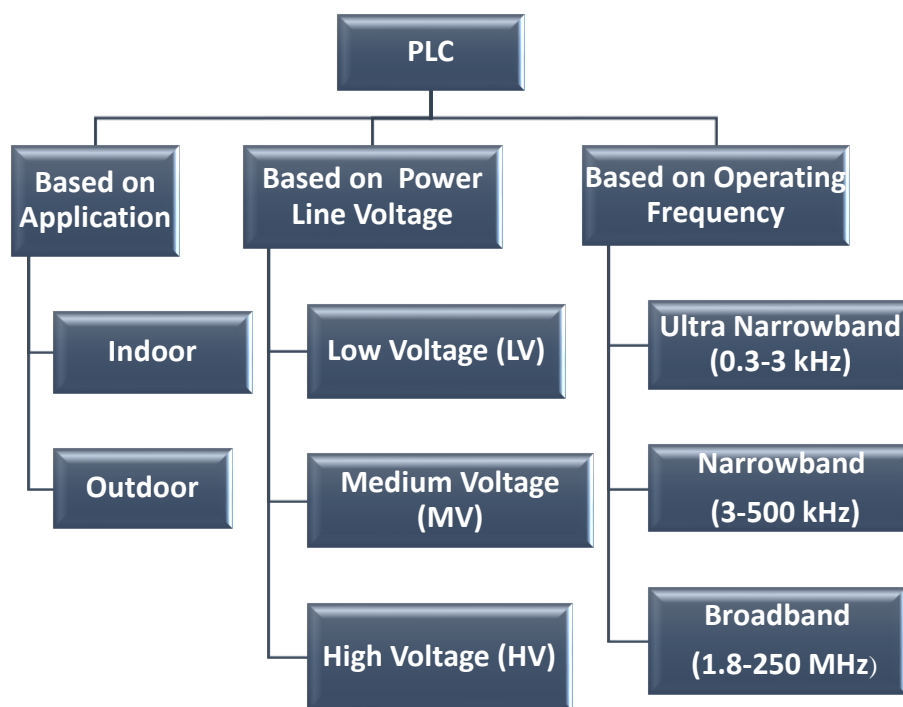

Fig. 2. Classification of PLC.

On the other hand, NB-PLC operates with low frequency of 3-500 kHz, and low data rates of up to hundreds kbps [10]. Due to its low frequency of operation, it is suitable for long distance telecommunication. Examples include communications between smart meters and data concentrators, which are deployed by local utilities on medium voltage (MV) or low voltage (LV) power lines [11]. Although the indoor channel is mainly employed by BB-PLC, there are still NB-PLC applications for home applications. Ultra-narrowband (UNB) PLC operates at very low data rate (hundred bps) but has very large operational range (hundreds of km). Hence, it is mostly employed for metering purposes across high voltage (HV), MV and LV levels. This research focuses on indoor LV PLC.

2.2. Types of Noise

There are several noise types that the PLC system is predisposed to. These noise types have been classified in the literature [12, 13], and are briefly discussed here as they form the focus for characterization in this research.

2.2.1. Colored Background Noise (CBGN)

This is a combination of conducted and coupled noise contributions [14]. The conducted noise accrue from devices connected to the power delivery network, while the coupled noise contributions are due to radio signals captured by the power line infrastructure. CBGN is caused by the summation of numerous noise sources with low power and relatively low power spectral density (PSD), which varies inversely with frequency.

2.2.2. Narrowband Noise (NBN)

This type of noise is mainly caused by broadcast radio signals that are coupled into the power line network through cables that are long enough to operate as antennas [15]. The bandwidths of NBN in narrowband have been reported to have an average value of about 3 kHz. At higher frequencies, these bandwidths can reach up to 10 kHz. The amplitude of NBN varies over the day time and becomes higher at night when reflection properties of the atmosphere become stronger [16].

2.2.3. Burst Noise (BN)

Any noise that is irregular in waveform shape is called burst noise. It is non-Gaussian in nature in the sense that it consists of sudden step-like transitions between two or more levels. It has characteristics similar to electrical noise from electrochemical processes, such as that observed in resistors and transistors and it is often associated with parameter drift. Each shift in offset voltage or current in burst noise can last for several milliseconds, and the intervals between pulses is less than 100 Hz. Impulsive noises that occur for long duration are also sometimes referred to as burst noise [17].

2.2.4. Continuous Noise

Continuous noise is a type of white noise with intensity of 89 dBc [18]. It is produced uninterruptedly by machinery that keeps operating without disturbance, such as factory equipment, heating or air-conditioning systems. Continuous noise is influenced by the quality of the power line infrastructure in the locality. Thus, the gravity of continuous noise is dependent on the nature of the power line environment itself, which could be low in some areas and higher in others. It could be measured for just a few minutes with a sound level meter to get a sufficient representation of the noise level.

2.2.5. Impulsive Noise

This is mostly related to the power frequency and it is introduced by load switching taking place on the line and, as a result, it is unpredictable. Impulsive noise is sub-divided into: aperiodic impulsive noise (APIN) and periodic impulsive noise (PIN). APIN is the primary noise component in BB-PLC and consists of short duration, high power impulses (up to 50 dB above background noise power). It occurs at random, although their duration fluctuates from some microseconds up to some milliseconds [19]. It is caused by switching transients in the network as a result of connection and disconnection of electrical devices. It could also result from interference of non-interoperable neighboring PLC modems.

Meanwhile, PIN exists in two forms: periodic impulsive noise synchronous with the mains (PINS) and periodic impulsive noise asynchronous with the mains (PINAS). PINS is also known as cyclostationary noise (CN) and it is dominant in NB-PLC. It is caused by power supplies like rectifier diodes, which occur synchronously with the mains frequency. They contain high peaks that occur for only short durations with repetition rate equal to or double that of the mains period, i.e., repetition rate of 50-100 Hz. On the other hand, PINAS have irregular occurrences in relation to the mains frequency and much higher repetition rates (50-200 kHz), hence they are unpredictable in nature [20, 21].

3.   REVIEW OF RELATED WORKS

Noise characterization in PLC involves the use of experimental procedures and measurements in order to establish the noise characteristics for various noise types peculiar to the PLC network [2, 22]. Noise characterization is also useful in categorizing different noise types and their sources for easier monitoring and handling. There are two approaches to perform noise characterization: i) by understudying the overall channel noise; and ii) by investigating the noise generated by end-user equipment. The latter could be carried out either by experimental activities carried out at the receiver modem, or at the port where the main sources of noise are connected. The first approach gives information about the overall noise in the system by examining the received signal and comparing it with the transmitted signal, while the second approach gives information about the level of disturbance each source injects into the system at certain point of the grid. In this research, the second approach is used. It has the following advantages: i) it provides a clear indication of devices that inject large noise components, and ii) it provides electromagnetic compatibility (EMC) regulation bodies with guidelines for the definition of electromagnetic emission limits to enable both using and the coexistence with PLC [21].

A statistical noise model (SNM) was developed for power line channel within 1-30 MHz in [23]. Noise measurements were taken on a real power line channel for selected appliances, from which the noise density spectrum (NDS) was obtained. The SNM was based on the probability density function (PDF) of the NDS. The measured noise was compared with that one simulated by the SNM. Similarly, Jiang et al. [24] proposed a scheme that combines the advantages of both the wavelet transform and the Wigner-Ville distribution (WVD) methods. Application of the proposed scheme to the signal measured from the real LV-PLC system, shows the effectiveness of the proposed method. Again, Han, et al. [12] proposed a field programmable gate array (FPGA)-based emulator to emulate power line noise scenarios flexibly in both narrowband and broadband.

In [15], the researchers presented a systematic approach to extract and parameterize each subtype of LV power line noise within 150 kHz and 10 MHz region. Different PLC noise types were extracted from the measurements using existing models such as linear switching time varying (LSTV) model, narrowband regression (NBR) model, multi-cyclic regression (MCR). The result of the characterization was used to develop an FPGA-based emulator to mimic the nature/characteristics of different PLC noise types examined in the research. Characterization of various types of PLC noise – CN, NB, and aperiodic noise – was carried out [14], taking measurements at the source.

Despite the existing works on this area, there is still room for development of further techniques towards addressing the problem. For example, the frequency domain analysis is carried out using the PSD obtained from the periodogram [25]. However, the use of this equipment has two major shortcomings: i) it cannot resolve sinusoids whose frequencies are separated by less than 1 cycle per time unit; and ii) it does not possess sufficient robustness against heavy-tailed noise such as outliers. In the present study, both time and frequency domain characterization of noise are done for 12 devices. The characterization process in this work is a combined approach of the PSD and time stream. PSD analysis is carried out on the captured noise signals using Welch's PSD estimation technique. Welch's method is employed to compute a modified periodogram for each segment and then average these estimates to produce the estimate of the PSD [26]. The method is computationally efficient due to its use of the fast Fourier transform (FFT).

In this study, two scenarios are considered for the noises captured from different devices. The scenarios are: noise generated during normal-mode operating condition of the appliance, and noise generated during transients. The three classes of electricity users' appliances are the focus in this research but there are other loads from the classes considered that could constitute higher noise sources to PLC systems even at LV level. The developed algorithm has the capability to characterize all noise types as against some existing algorithms that are meant for characterizing only one type of noise.

4. EXPERIMENTAL SETUP FOR DATA CAPTURING

The schematic block diagram of the measurement setup is shown in Fig. 3(a) while the real setup for an appliance is shown in Fig. 3(b). This configuration is adopted for each of the appliances considered in this study. The power supply network is the electricity power supply source. A low-pass filter is used to isolate the device under test (DUT) from the rest of the power delivery network. The DUT is the device whose noise characteristics are to be captured on a single-phase LV power line. Data capturing was carried out on different power lines since all the DUTs could not be obtained in one place.

A PLC coupler is placed just before the digital storage oscilloscope (DSO) for protection. It acts as a band-pass filter to isolate the DSO from the low frequency mains voltage which is of high amplitude (220-240 V). At the same time, it functions as a ratio 1:1 transformer by allowing all the components of higher frequency signals to pass through. It is this high frequency signals that are to be captured as the noise. The DSO is the device that captures the noise signals from the LV lines to which the DUT is connected, and stores the data. The devices selected for experimental consideration for this research and ratings are outlined in Table 1.

The specifications of the DSO are as follows:
- Input impedance: 1 MΩ/30 pF.
- Maximum input voltage: 30 V (AC+DC).
- Input range: 10 mV – 3V/Division.
- Record length: 4000 samples/channel.
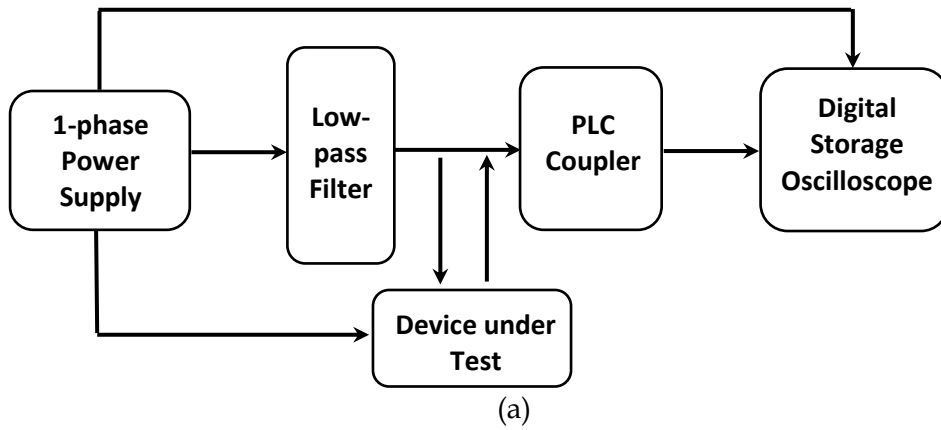- Sampling Frequency: 250 Hz – 25 MHz.

(a)

(b)

Fig. 3. Experimental setup for a device under test: a) schematic diagram; b) actual setup.

Table 1. Sampled devices and ratings.

Device	Rating	Load class
Air conditioner	Current: 5.7 A Power coupling: 1260 W	Residential
Desktop PC	Power: 1020 W	
Light dimmer incandescent	Power: 60 W	
Standing fan	Power: 125 W	
Laptop	Power: 130 W	
Pressing iron	Power: 1000 W	
Satellite decoder	Power: 15 W	
LCD television	Power: 85 W	
Printer	Current: 4 A	Commercial
Hair dryer	Power: 2000 W	
Photocopier	Power: 1200 W	
Welding machine	Capacity: 10.4 kVA Welding current: 151 A	Industrial

The PLC coupler used is STEVAL – XPLM01CPL. It is a PLC alternating current (AC) coupling circuit. It is simple, yet very useful for PLC testing. The specifications for the low-pass filter are as follows:

- Maximum line-to-ground leakage current: 0.25 mA at 115 VAC 60 Hz and 0.45 mA at 250 VAC 50 Hz.
- Hipot rating (one minute): 1450 VDC line-to-ground and 2250 VDC line-to-line.
- Operating frequency: 50/60 Hz.
- Rated voltage: 115/250 VAC.

5. SIGNAL ANALYSIS AND NOISE CHARACTERIZATION ALGORITHM

The proposed algorithm in this study was coded in MATLAB. The algorithm is divided into two stages: noise signal analysis and parameters determination; and noise characterization. Details of each are discussed in the following subsections.

5.1. Noise Signal Analysis

This stage of the algorithm involves spectral analysis of the noise signals. The goal of spectral analysis is to decompose the noise signal data into a sum of weighted sinusoids. This process enables assessing the frequency content of the phenomenon under study, which may be concentrated in some narrow frequency band or might be spread across a broad range of frequencies. Spectral analysis is divided into two major areas: Fourier transform and PSD.

In this study, the signals are analyzed using the Welch PSD estimation method [26]. This is an approach for estimating the power of a signal at different frequencies. It is based on the concept of using periodogram spectrum estimates, which would result in converting a signal from time domain to frequency domain.

Performing the spectral analysis on a computer begins with a sequence of data values or samples. So, given a discrete-time signal $y(t)$; $t = 0, \pm1, \pm2\ldots$, assumed to be a sequence of random variables measured in volts. The Fourier transform of the signal $y(t)$ is given as:

$$Y(f) = \int_{-\infty}^{\infty} y(t)\, e^{-j2\pi ft}\, dt \qquad [\text{V/Hz}] \tag{1}$$

To recover the original signal $y(t)$ from Eq. (1), the inverse Fourier transform of the expression in Eq. (1) is computed as presented in Eq. (2).

$$y(t) = \frac{1}{2\pi} \int_{-\infty}^{\infty} Y(f)\, e^{j2\pi ft}\, df \qquad [\text{V}] \tag{2}$$

By the convolutional theorem, the Fourier transform of $y(t)$ is $Y(f)*Y(f)$; is expressed as:

$$\int_{-\infty}^{\infty} y^2(t)\, e^{-j2\pi ft}\, dt = \int_{-\infty}^{\infty} Y(f)Y(\tau - f)\, df \tag{3}$$

Note that $Y(f)=Y^*(-f)$ since $y(t)$ is a real function. Setting $\tau = 0$ in Eq. (3) yields:

$$\int_{-\infty}^{\infty} y^2(t)\, dt = \int_{-\infty}^{\infty} Y(f)Y(-f)\, df = \int_{-\infty}^{\infty} |Y(f)|^2\, df \tag{4}$$

Eq. (4) is the Parseval's theorem, which states that "the total power in a waveform computed in the time domain is the same as the total power computed in the frequency domain". Therefore, the total power (*TP)* is obtained as:

$$TP = \int_{-\infty}^{\infty} y^2(t)dt \tag{5}$$

Supposing $y(t)$ is time-limited such that $-\frac{T}{2} < t < \frac{T}{2}$, then Eq. (4) becomes:

$$\int_{-\frac{T}{2}}^{\frac{T}{2}} y^2(t)dt = \int_{-\infty}^{\infty} |Y(f)|^2 \, df \tag{6}$$

Therefore the average power of y(t) is:

$$P_y = \frac{1}{T}\int_{-\frac{T}{2}}^{\frac{T}{2}} y^2(t)dt = \int_{-\infty}^{\infty} \frac{1}{T}|Y(f)|^2 \, df \tag{7}$$

Hence, the PSD of $y(t)$ is defined by Eq. (8a).

$$PSD = P_y(f) = \frac{1}{T}|Y(f)|^2 \tag{8a}$$

Eq. (8b) is the average power spectral density of the noise captured from the network when DUT is connected while Eq. (8c) is the power spectral density of the background noise only, where 1/T is the sampling frequency, F_S.

$$PSD_{D\&BN} = P_x(f) = \frac{1}{T}|X(f)|^2 \tag{8b}$$

$$PSD_{BGN} = P_g(f) = \frac{1}{T}|G(f)|^2 \tag{8c}$$

The PSD of the noise generated by the DUT, called the device effective noise PSD, PSD_{DEN}, is then calculated as:

$$PSD_{DEN} = PSD_{D\&BN} - PSD_{BGN} \tag{9}$$

where $PSD_{D\&BN}$ is the PSD of the noise recorded on the network line while the DUT is connected, PSD_{BGN} is the line background noise without DUT connection.

Eq. (10) is presented to compute the slope, m, of the PSD plot, while Eq. (11) calculates the repetition rate and Eq. (12) computes the segment acquisition time.

$$m = \frac{(PSD_U^{DEN} - PSD_L^{DEN})}{(Freq_U - Freq_L) \times 10^{-6}} \tag{10}$$

$$RR = \frac{1}{(DT + SAT)} \tag{11}$$

$$SAT = \frac{RL}{F_s} \tag{12}$$

where SAT is the segment acquisition time, DT is the dead time of the DSO, RL is the DSO record length, and F_S is the sampling frequency. Considering that the signal is in volts, the PSD which gives the information of how the variance is distributed amongst the various frequency components has units of V^2/Hz.

In this study, a MATLAB tool called *pwelch*, is employed to compute the PSD of the captured noise signals as illustrated in Fig. 4. From the PSD plot, the slope (m) and bandwidth (BW) in kHz are obtained. Other parameters such as impulse amplitude (A_i) in volts, impulse width/duration (t_i) in μs, and repetition rate (RR) in kHz are obtained from the time stream of the signals using MATLAB function. Fig. 4 presents the flowchart for signal analysis using PSD and determination of noise parameters, which is implemented in

MATLAB to generate both the PSD, plotted in Figs. 6-11 and the values exhibited in Table 2 where:

$g(t)$ – Background noise

$x(t)$ – Background and DUT noises

t – time

BW_{ave} – Average Bandwidth

$P_y(f)$ – PSD of a given signal $y(t)$

F_s – sampling frequency = 10 MHz

$P_{D\&BN}$ – Average PSD for Background plus DUT noise

P_{BGN} – Average PSD for background noise

RR – Repetition rate

A_i – Impulse amplitude

t_i – Impulse duration

m – Slope of the PSD plot

$Freq_U$ – Upper bound frequency

$PSD^{DEN}{}_L$ – Lower bound of PSD_{DEN}

$PSD^{DEN}{}_U$ – Upper bound of PSD_{DEN}

BW_L - Lower bound of the BW

BW_U - Upper bound of the BW

N, M – Lower and Upper limits for NBN

V, W – Lower and Upper limits for PIN

Q, R, S, T – Test parameters for repetition rate

DT – DSO dead time = 400 ns

RL – DSO record length

$Freq_L$ – Lower bound frequency and parameter values are:

N = 3 kHz; M = 10 kHz; Q = 50 kHz;

R = 100 kHz; S = 200 kHz; T = 100 ms;

V = 50 MHz; W = 100 MHz;
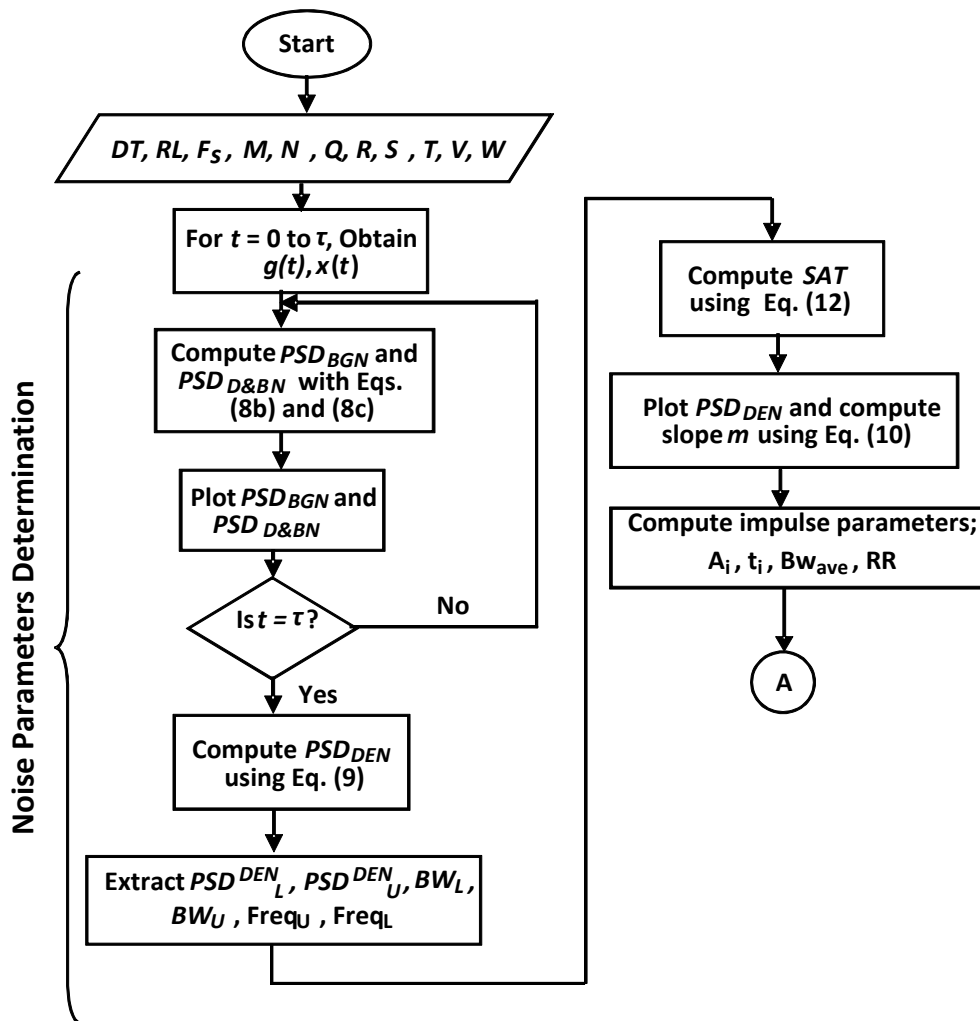
RL = 4000 samples/channel

Fig. 4. Flowchart for signal analysis and noise parameters determination.

5.2. Noise Characterization Algorithm

In this stage of the proposed algorithm, noise characterization is performed. The parameters obtained from Section 5.1 are used in conjunction with certain thresholds obtained from the literature, to characterize the noise signals. The output of the characterization process gives the noise type obtained from the signals. The flowchart to implement the noise characterization is shown in Fig. 5.
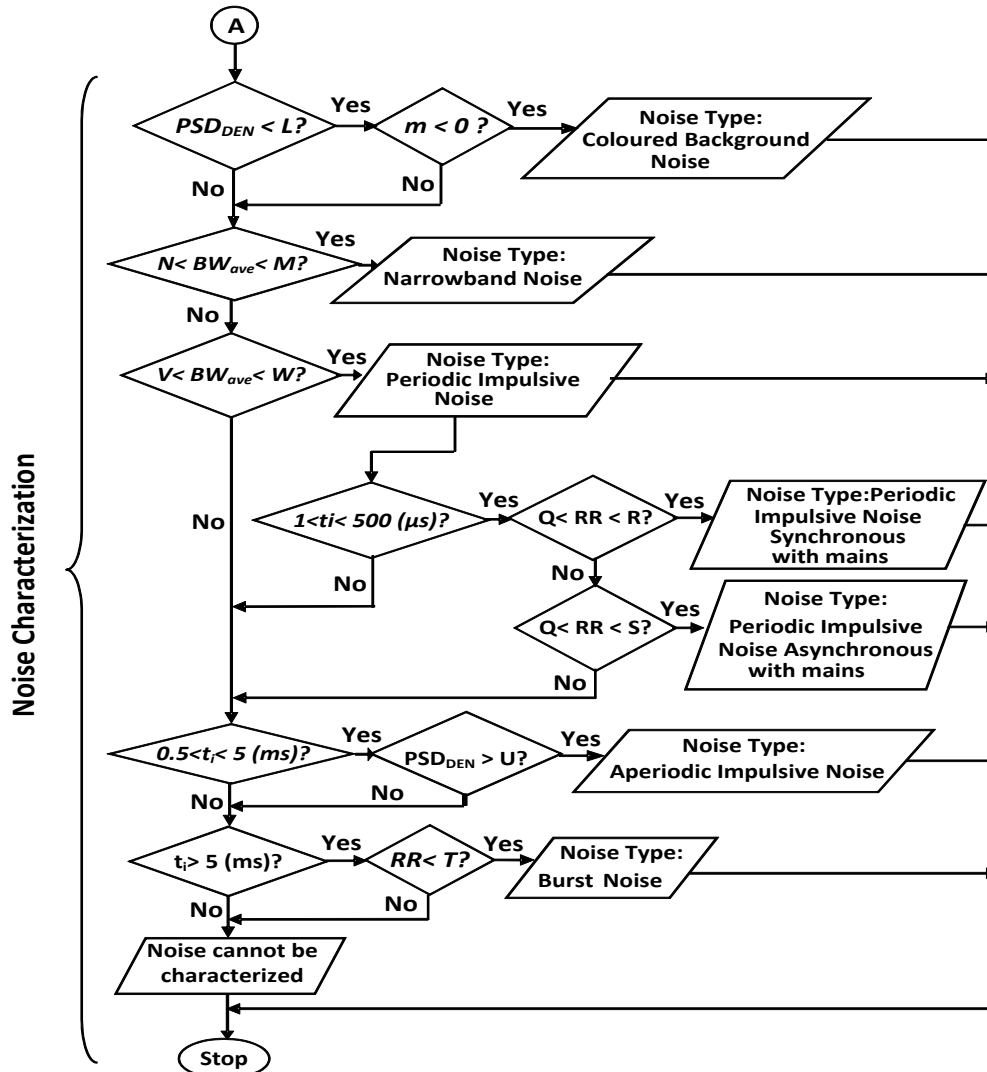

Fig. 5. Flowchart for the noise signal characterization.

6. RESULTS AND DISCUSSION

In this section, reports on the results obtained from the noise analysis and characterization process are presented and discussed. Though twelve DUTs are examined in the study, the results of six DUTs are presented and discussed in the paper due to space constraint. The two scenarios considered in the study are: at the instance of switching of the device and when it was running. Noise generated by DUT in time domain and the spectral analysis of the captured noise signals (background and DUT) are presented for each of the DUTs for both scenarios. Furthermore, the characterization parameters obtained from the analysis as well as the output of the process (the noise type) are also presented.

6.1. DUT 1: Welding Machine

Fig. 6 shows noise signals from a welding machine and PSD analysis. Figs. 6(a) and 6(b) show the noise signal and the PSD of the medium called background noise, where the average PSD is -101.60 dB/Hz. It is observed to be denser compared to that obtained for most of the measured devices. Figs. 6(d) and 6(f) illustrate the PSD of the DUT and background noise at the instance of switching and in running mode, respectively. It is observed that the peak PSD of the noise at switching is -69 dB/Hz at 0.4 MHz and the lowest of -102 dB/Hz is obtained at a frequency of 4.2 MHz. This brings an average value of -14.66 dB/Hz shown in Table 2 for the DUT alone. The running mode of the machine obtains the same peak and lowest PSD values but only at different frequency.
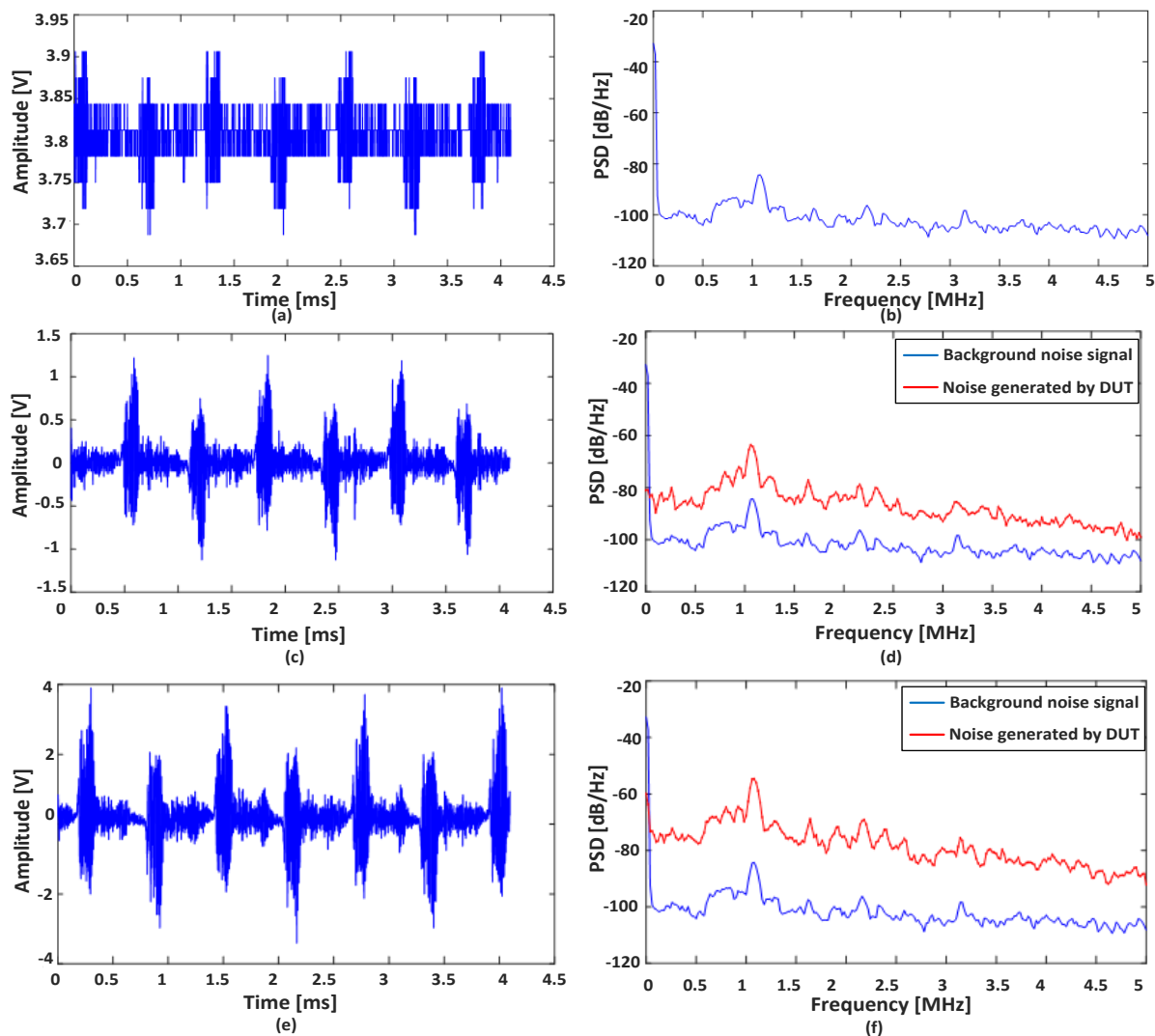

Fig. 6. Noise signals from a welding machine and PSD analysis: a) measured background noise signal; b) PSD analysis of background noise; c) measured noise signal (switch on); d) PSD analysis of noise (switch on); e) measured noise signal (running); f) PSD analysis of noise (running).

However, an average value of -23.36 dB/Hz is obtained for the machine during operation. This shows that more noise is added to the system at the instance of switching. On the other hand, repetition rates of 115.63 kHz and 122.70 kHz are obtained for the machine at the instance of switching and in operation, respectively. To sum it up, the noise generated by this machine is characterized as PINAS.

6.2.   DUT 2: Satellite Decoder and LCD Television

In this case, a combined load source of a satellite decoder and an LCD television is investigated. Fig. 7 illustrates the noise signals and the PSD analysis for different scenarios. The average PSD of the noise from the combination - as shown in Table 2 - are -4.94 dB/Hz and -3.92 dB/Hz for switching and running operations, respectively. Since the value of the latter is greater than the former, it means that more noise is injected during the operation mode than at instance of switching. The values obtained for the satellite decoder and television separately are -4.36 dB/Hz and -3.21 dB/Hz, respectively for the switching mode whereas -3.96 dB/Hz and -3.86 dB/Hz are, respectively, obtained for the running mode. The revelation here is that the television invokes more noise than a combination of the two during the switching operation. Nevertheless, the output of the characterization process of the combined noise source did not produce so much difference in the noise type from that obtained when the decoder and television were measured separately. The noise was yet obtained to be PINS.
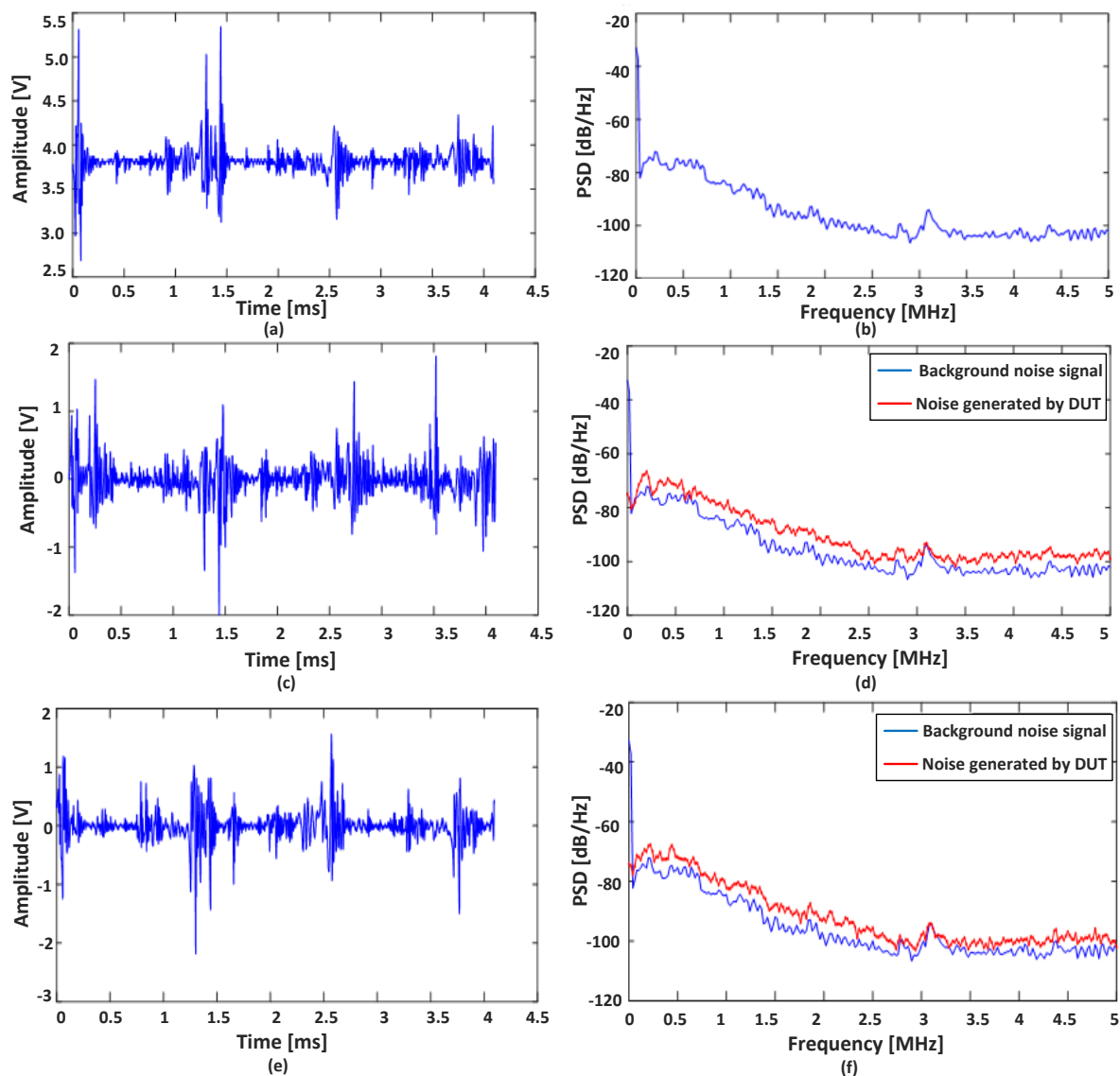
Fig. 7. Noise signals from a satellite decoder and an LCD television and PSD analysis: a) measured background noise signal; b) PSD analysis of background noise; c) measured noise signal (switch on); d) PSD analysis of noise (switch on); e) measured noise signal (running); f) PSD analysis of noise (running).

6.3. DUT 3: Laptop

Fig. 8 shows noise signals from a laptop in addition to the PSD analysis. The average values of PSD of the noise signal, captured from this device are -8.22 dB/Hz and -3.66 dB/Hz for switching and running modes, respectively. This clearly shows that more noise is generated during the running mode. This is observed from Fig. 8(f) that there are sudden rises in the noise generated by the DUT between 2.5 - 3.7 MHz frequency region. This indicates that signals transmitted within this frequency range are likely to encounter noise if a laptop is on the same power line at the time of transmission.
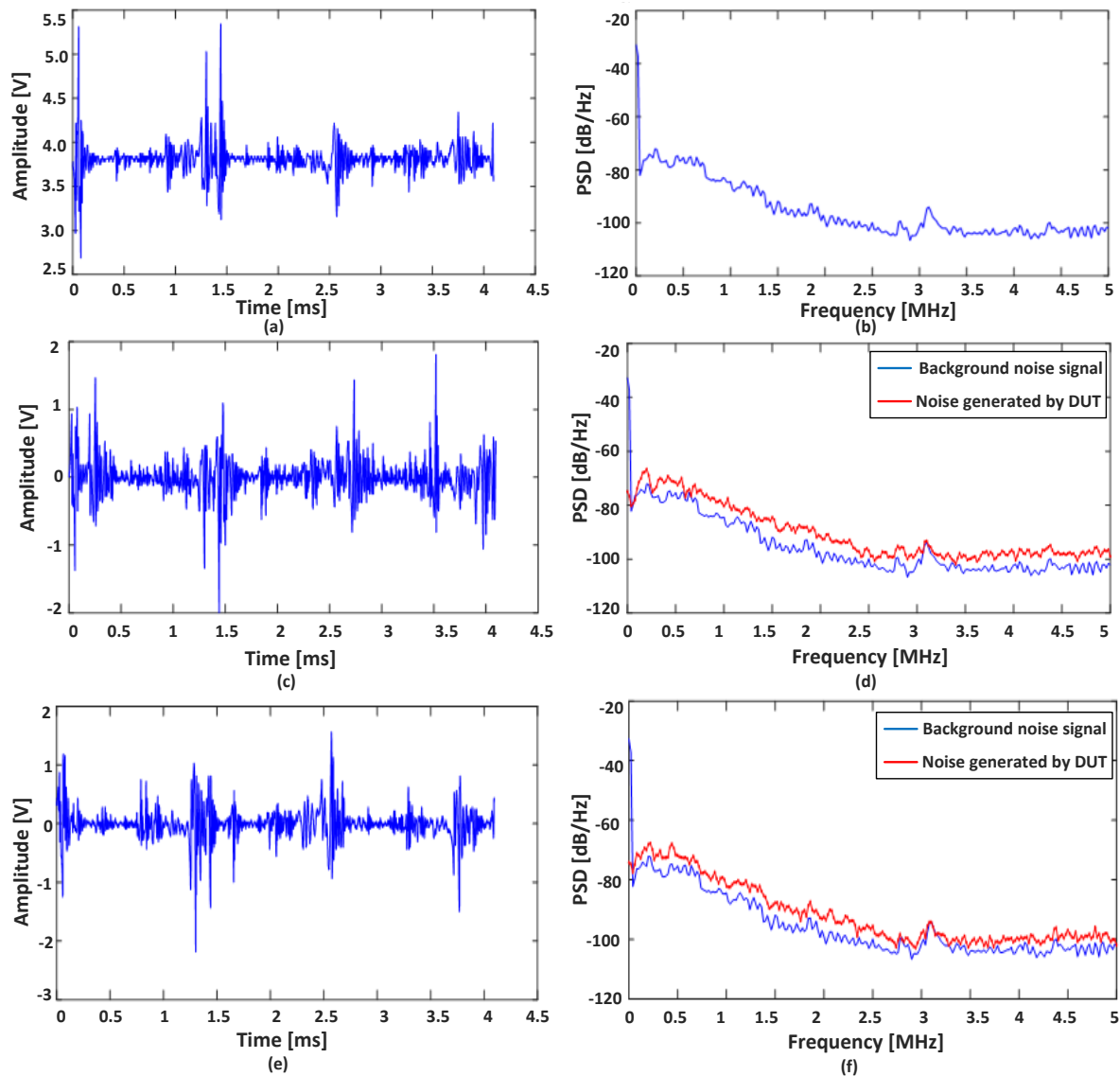
Fig. 8. Noise signals from a laptop and PSD analysis: a) measured background noise signal; b) PSD analysis of background noise; c) measured noise signal (switch on); d) PSD analysis of noise (switch on); e) measured noise signal (running); f) PSD analysis of noise (running).

The output of the characterization process gave the noise type as PINS with the impulse repetition rate of 80 kHz in the switching case. On the other hand, the impulse repetition rate - as shown in Table 2 - leveled up to 214.93 kHz in the running mode. Because of this high value that exceeds the limit for repetition rate of 200 kHz for PINAS as reported in the literature, the algorithm could not characterize the noise. Therefore, the output of the

characterization process is "cannot be characterized". Despite the stated reason, the authors feel that the noise obtained during the running mode may be PINAS since the value is close to the threshold.

6.4.   DUT 4: Hair dryer

Fig. 9 shows the noise signals from a hair dryer and the PSD analysis. The noise signals generated, by the hair dryer appear to have lots of shoot-ups and also seem to be periodic in nature. However, from the PSD analysis plot, it is observed that the noise power difference is high. The average PSD of the noise from the DUT in the switching mode is -2.84 dB/Hz and -2.94 dB/Hz for the running mode. This is the highest value obtained so far indicating that that the dryer contributes significant noise to the network. In addition, it is observed that the noise spikes had increased in number, which indicates that the repetition rate of the impulses has increased. The device noise is characterized as CBGN. This is seen from comparing PSD analysis of noise at switch-on and measured noise signal at running.
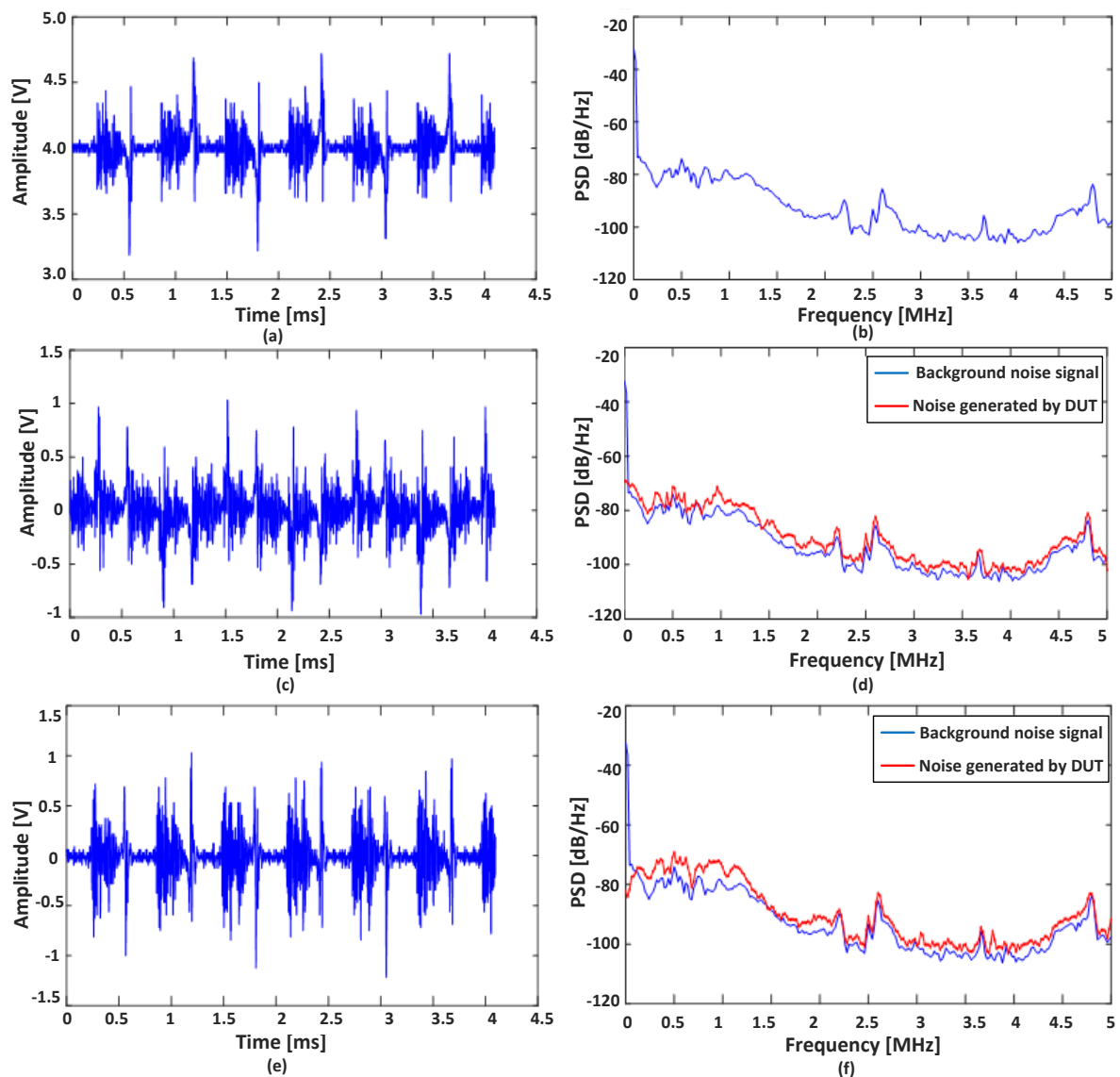

Fig. 9. Noise signals from a hair dryer and PSD analysis: a) measured background noise signal; b) PSD analysis of background noise; c) measured noise signal (switch on); d) PSD analysis of noise (switch on); e) measured noise signal (running); f) PSD analysis of noise (running).

6.5. DUT 5: Photocopier

Fig. 10 shows noise signals from a photocopier and PSD analysis. From Fig. 10(c), it is observed that the noise has a repetitive outlook. This is confirmed from the noise characterization process, the noise type is PINS. During the running mode, the average noise power for the DUT increased from -4.12 dB/Hz at switch on mode to -2.24 dB/Hz during the running mode. The noise is, therefore, characterized as CBGN in the running mode whereas it is classified as PINS in the switching mode. It can be concluded that the noise generated by the photocopier is higher during switch on operation. The parameters obtained from the algorithm that was used for the characterization are displayed in Table 2.
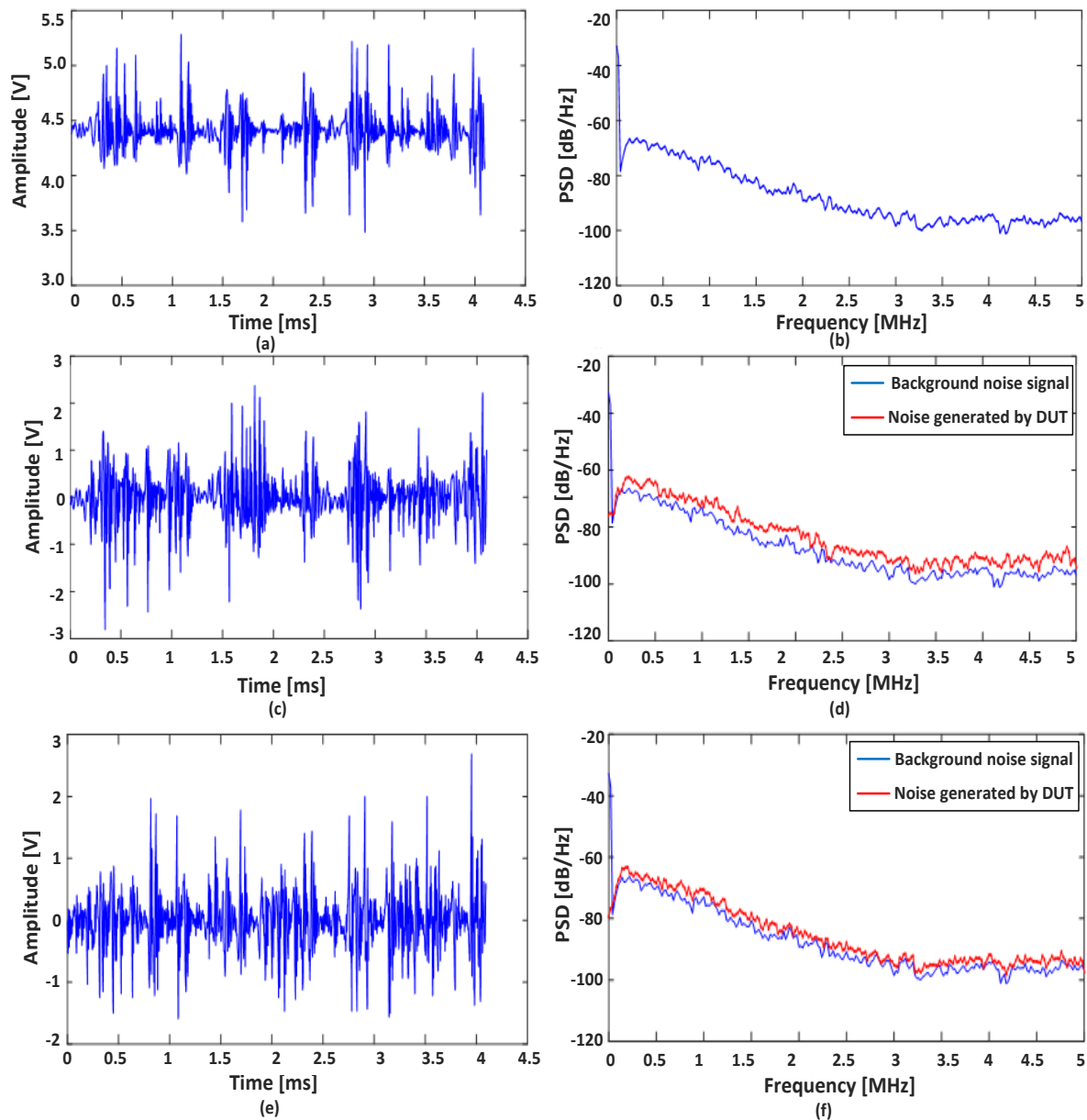

Fig. 10. Noise signals from a photocopier and PSD analysis: a) measured background noise signal; b) PSD analysis of background noise; c) measured noise signal (switch on); d) PSD analysis of noise (switch on); e) measured noise signal (running); f) PSD analysis of noise (running).

6.6.   DUT 6: Light Dimmer

Fig. 11 shows noise signals from a light dimmer and PSD analysis. Figs. 11(a) and 11(b) are the time domain and frequency domain plots of the background noise, respectively. Figs. 11(c) and 11(d) gives the corresponding plots for the light dimmer while running at quarter power. Observing Fig. 11 (c), the dimmer lamp appeared to have so many shoot ups, but just like the case of the laptop, the PSD analysis shown in Fig. 11 (d) reveals that the noise power for the DUT is -2.36 dB/Hz. Hence the noise is characterized as CBGN. The dimmer lamp was then turned to half rated power. In this case, the noise average PSD reduced to -3.73 dB/Hz. In this case, the obtained noise is classified as PINS. This happens because they both have impulse repetition rate of 72.47 kHz and 76.25 kHz, respectively for characterization as CBGN and PINS.
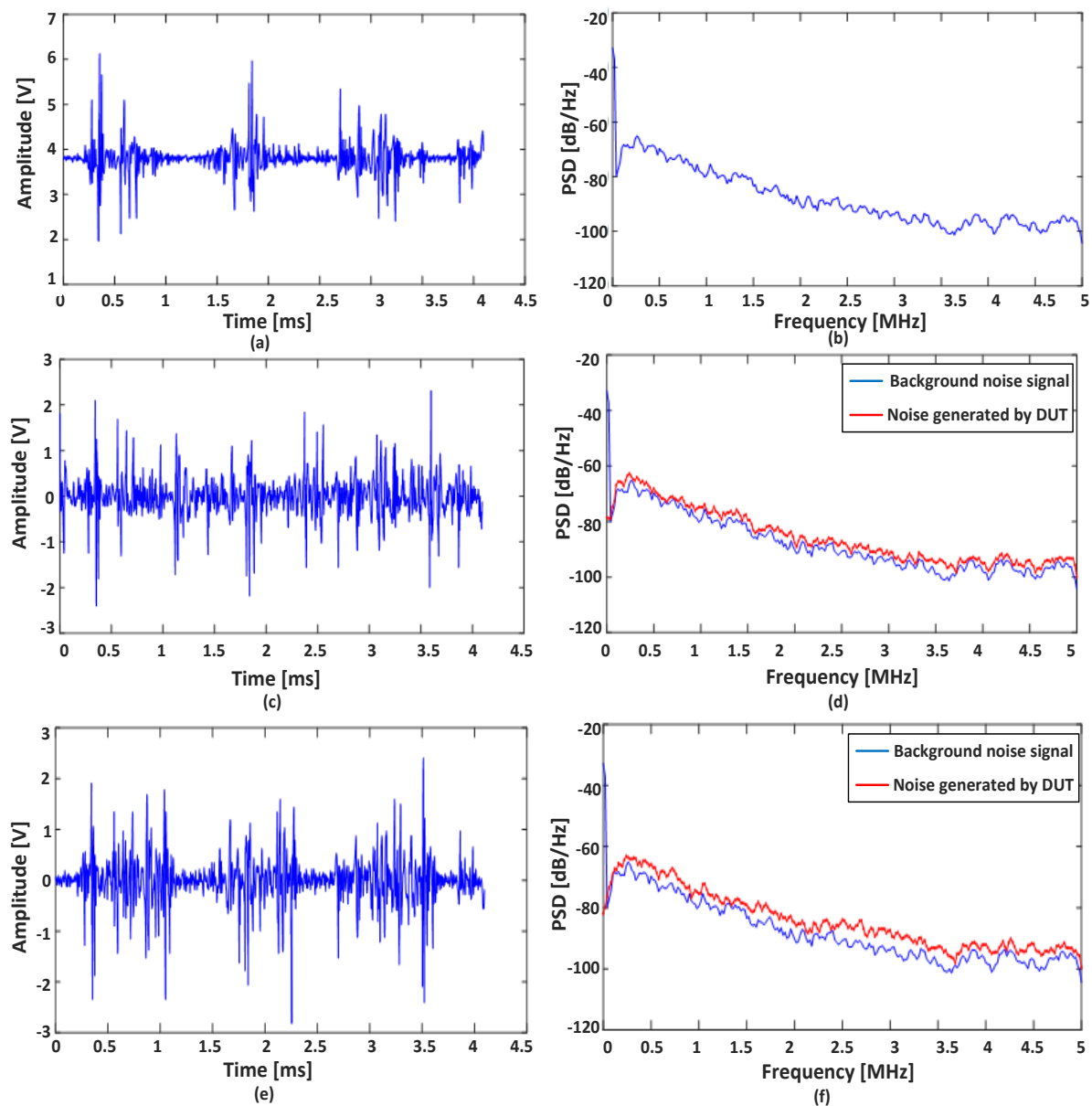
Fig. 11. Noise signals from a light dimmer and PSD analyses: a) measured background noise signal; b) PSD analysis of background noise; c) measured noise signal (switch on); d) PSD analysis of noise (switch on); e) measured noise signal (running); f) PSD analysis of noise (running).

It should be noted that narrowband noise was not obtained from any of the DUTs. This is, perhaps, due to the fact that none of the devices considered in this study contained transmitters and/or receivers. This conclusion is supported by two of the existing works [11] and [27] that state that electrical appliances that contain transmitters or receivers are likely to generate NBN.

Table 2. Characterization parameters of the noise, generated by various DUTs.

| DUT | Operating mode | Characterization parameters | | | | | | | Noise type |
		PSD_{BGN} [dB/Hz]	$PSD_{D\&BN}$ [dB/Hz]	PSD_{DEN} [dB/Hz]	BW [MHz]	m [x10⁻³]	t_i [µs]	RR [kHz]	
HRD	Switch on	-92.74	-89.90	-2.84	4.7951	-1.30	6.013	116.73	CBGN
	Running	-92.74	-89.80	-2.94	4.7385	-1.30	6.393	133.58	CBGN
LPC	Switch on	-95.68	-87.46	-8.22	3.4757	-1.20	12.881	80.01	PINS
	Running	-95.68	-92.02	-3.66	3.7087	-1.70	7.416	214.93	*CBC
WDM	Switch on	-101.60	-86.94	-14.66	4.1839	-0.22	4.613	115.63	PINAS
	Running	-101.60	-78.24	-23.36	4.0867	-0.13	5.856	122.70	PINAS
STD	Switch on	-95.25	-90.89	-4.36	2.9807	-1.80	13.774	62.37	PINS
	Running	-95.25	-91.29	-3.96	2.8563	-1.70	11.586	92.72	PINS
LCD television	Switch on	-95.25	-92.04	-3.21	2.9125	-2.10	13.307	73.88	PINS
	Running	-95.25	-91.39	-3.86	3.0819	-1.80	12.234	65.60	PINS
SD&T	Switch on	-95.25	-90.31	-4.94	3.0327	-1.90	10.602	75.39	PINS
	Running	-95.25	-91.33	-3.92	2.4450	-1.80	8.954	96.55	PINS
Photoco-pier	Switch on	-87.37	-83.25	-4.12	3.0854	-1.70	12.781	72.40	PINS
	Running	-87.37	-85.13	-2.24	2.7302	-1.80	11.813	67.28	CBGN
Light dimmer	Running 1	-87.80	-85.44	-2.36	2.9743	-1.40	14.508	72.47	CBGN
	Running 2	-87.80	-84.07	-3.73	3.0619	-1.30	12.235	76.25	PINS

where HRD = hair dryer; LPC = laptop PC; WDM = welding machine; STD = satellite decoder; SD&T = satellite decoder and LCD television; *CBC = cannot be characterized.

7. CONCLUSIONS

Through measurements carried out on real-life indoor power line networks, different noise characteristics were investigated. An algorithm for characterizing the noise generated by end-user equipment of a power distribution system was presented in this paper. The characterization process was a combined approach of the PSD and time stream. PSD analysis was carried out on the captured noise signals using the Welch's PSD estimation technique. In the study, both time and frequency domain characterization of noise were done for 12 devices being selected for the study. The results obtained were evaluated against previous works. From the results, the laptop, photocopier, light dimmer, and hair dryer were found to be the noisiest devices, while the welding machine did not inject much noise. This is really contrary to the impression one would have had about the device.

It was also observed that more devices on the network provoked higher noise effects. The light dimmer was very noisy and exhibited periodic impulsive noise synchronous with the mains. It was also observed that the photocopier in the running mode injected the highest level of noise with an average PSD value obtained as -2.24 dB/Hz. The combination of a

satellite decoder and an LCD television also contributed in no small measure to the amount of noise generated by the DUTs.

On a whole, the developed algorithm in this study was able to characterize the noise signals captured from the DUTs into three types; CBGN, PINS, and PINAS. The method is computationally efficient due to its use of the FFT. However, continuous noise was not characterized in this work, probably due to the use of low-pass filter. Similarly, NB, APIN and BN were not obtained from any of the devices considered. This may be due to the frequency of operation (25 MHz) of the digital storage oscilloscope used for the measurements, on which further studies will focus.

REFERENCES

[1] S. Shebl, N. Soliman, N. El-Fishawy, A. Abou-El-Azm, S. Alshebeili, F. El-Samie, "Performance enhancement of power line communication systems with efficient low density parity-check codes, noise removal, equalization, and chaotic interleaving," *Digital Signal Processing*, vol. 23, no. 6, pp. 1933-1944, 2013.

[2] G. Artale, A. Cataliotti, V. Cosentino, D. Di Cara, R. Fiorelli, S. Guaiana, N. Panzavecchia, G. Tine, "A new PLC-based smart metering architecture for medium/low voltage grids: feasibility and experimental characterization," *Measurement: Journal of the International Measurement Confederation*, vol. 129, pp. 479-488, 2018.

[3] G. Artale, A. Cataliotti, V. Cosentino, D. Di Cara, R. Fiorelli, S. Guaiana, N. Panzavecchia, G. Tine, "A new coupling solution for G3-PLC employment in MV smart grids," *Energies*, vol. 12, no. 13, pp. 2474, 2019.

[4] A. Garg, A. Gill, "Designing reliable power-line communications," *Electrical Design News*, vol. 55, no. 23, pp. 24, 2019.

[5] S. Galli, A. Scaglione, Z. Wang, "For the grid and through the grid: the role of power line communications in the smart grid," *Proceedings of the IEEE*, vol. 99, no. 6, pp. 998-1027, 2011.

[6] A. Amarsingh, H. Latchman, D. Yang, "Narrowband power line communications: enabling the smart grid," *IEEE Potentials*, vol. 33, no. 1, pp. 16–21, 2014.

[7] M. Elgenedy, M. Sayed, N. Al-Dhahir, R. Chabaan, "Temporal-region-based cyclostationary noise mitigation for SIMO powerline communications," *IEEE International Conference on Communications*, Kansas City, MO, pp. 1-6, 2018.

[8] H. Dai, H. Poor, "Advanced signal processing for powerline communications," *IEEE Communications Magazine*, vol. 41, no. 5, pp. 100-107, 2003.

[9] M. Giraneza, M. Kahn, "Broad band opto-capacitive power line communication coupler for DC nanogrids," *Journal of King Saud University-Engineering Sciences*, vol. 32, no. 4, pp. 246-254, 2020.

[10] P. Mlynek, R. Fujdiak, J. Misurec, J. Slacik, "Experimental measurements of noise influence on narrowband power line communication," *8th International Congress on Ultra-Modern Telecommunications and Control Systemsand Workshops*, Lisbon, pp. 94-100, 2016.

[11] J. Lin, M. Nassar, B. Evans, "Impulsive noise mitigation in powerline communications using sparse bayesian learning," *IEEE Journal on Selected Areas in Communications*, vol. 31, no. 7, pp. 1172-1183, 2013.

[12] B. Han, V. Stoica, C. Kaiser, N. Otterbach, K. Dostert, "Noise characterization and emulation for low-voltage power line channels across narrowband and broadband," *Digital Signal Processing*, vol. 69, pp. 259-274, 2017.

[13] B. Han, V. Stoica, C. Kaiser, N. Otterbach, K. Dostert, "Noise characterization and emulation for low-voltage power line channels between 150 kHz and 10 MHz," *Karlsruher Institut für Technologie*, pp. 3-15, 2016.

[14] R. Hashmat, *Characterization and Modeling of the Channel and Noise for Indoor MIMO PLC Networks*, PhD Thesis, Télécom Bretagne, Université de Rennes, France, 2012.

[15] M. Antoniali, F. Versolatto, A. Tonello, "An experimental characterization of the PLC noise at the source," *IEEE Transactions on Power Delivery*, vol. 31, no. 3, pp. 1068-1075, 2016.

[16] K. Anju, Y. Shyju, "Noise study in the integrated system of power line communication and visible light communication," *International Journal of Innovative Research in Computer and Communication Engineering*, vol. 3, no. 8, pp. 7912-7917, 2015.

[17] P. Lopes, J. Gerald, "Improving bit error rate under burst noise in OFDM power line communications," *Digital Signal Processing*, vol. 51, pp. 47-53, 2016.

[18] S. Dornic, T. Laaksonen, "Continuous noise, intermittent noise, and annoyance," *Perceptual and Motor Skills*, vol. 68, no. 1, pp. 11–18, 1989.

[19] L. Bai, M. Tucci, S. Barmada, M. Raugi, T. Zheng, "Classification and characterization of impulsive noise on indoor power line communications," *Energies*, vol. 11, no. 4, pp. 863, 2018.

[20] M. Mosalaosi, *Power Line Communication (PLC) Channel Measurements and Characterization*, Master thesis, University of Kwazulu-natal, Kwazulu-natal, South Africa, 2014.

[21] I. Fernández, M. Alberro, J. Montalbán, A. Arrinda, I. Angulo, D. de la Vega, "A new voltage probe with improved performance at the 10 kHz–500 kHz frequency range for field measurements in LV networks," *Measurement: Journal of the International Measurement Confederation,* vol. 145, pp. 519-524, 2019.

[22] A. Llano, D. De La Vega, I. Angulo, L. Marron, "Impact of channel disturbances on current narrowband power line communications and lessons to be learnt for the future technologies," *IEEE Access*, vol. 7, pp. 83797-83811, 2019.

[23] A. Voglgsang, T. Langguth, G. Korner, H. Steckenbiller, R. Knorr, "Measurement characterization and simulation of noise on powerline channels," *International Symposium on Power Line Communications and its Applications*, Limerick, Germany, pp. 139-146, 2000.

[24] X. Jiang, J. Nguimbis, S. Cheng, H. He, X. Wu, "A novel scheme for low voltage powerline communication signal processing," *International Journal of Electrical Power and Energy Systems*, vol. 25, no. 4, pp. 269-274, 2003.

[25] T. Li, "A robust periodogram for high-resolution spectral analysis," *Signal Processing*, vol. 90, no. 7, pp. 2133-2140, 2010.

[26] O. Solomon Jr, "PSD computations using Welch's method," *STIN 92*, pp. 23584, 1991.

[27] J. Cortes, L. Diez, F. Canete, J. Sanchez-Martınez, "Analysis of the indoor broadband power-line noise scenario," *IEEE Transactions on Electromagnetic Compatibility*, vol. 52, no. 4, pp. 849–858, 2010.